In presenting the dissertation as a partial fulfillment of the requirements for an advanced degree from the Georgia Institute of Technology, I agree that the Library of the Institute shall make it available for inspection and circulation in accordance with its regulations governing materials of this type. I agree that permission to copy from, or to publish from, this dissertation may be granted by the professor under whose direction it was written, or, in his absence, by the Dean of the Graduate Division when such copying or publication is solely for scholarly purposes and does not involve potential financial gain. It is understood that any copying from, or publication of, this dissertation which involves potential financial gain will not be allowed without written permission.

7/25/68

DESIGN AND ANALYSIS OF A DAMPED ESCAPEMENT MECHANISM

A THESIS

Presented to

The Faculty of the Division of Graduate

Studies and Research

by

Kantilal Nanji Gada

In Partial Fulfillment

of the Requirements for the Degree

Master of Science in Mechanical Engineering

Georgia Institute of Technology

September 1970

DESIGN AND ANALYSIS OF A DAMPED ESCAPEMENT MECHANISM

Approved:

Chairman

Date Approved by Chairman: August 27, 1970

ACKNOWLEDGEMENTS

The author wishes to express the deepest gratitude to Dr. J. R. Baumgarten for his enthusiasm and ability to suggest new methods and ideas. This work could not have been successfully undertaken without his suggestions and advice.

Appreciation is extended to Dr. C. V. Smith and Dr. J. H. Murphy for serving on the reading committee and for reviewing the manuscript.

Indebtness is expressed to Mr. R. G. Grim for his willingness to aid in solving problems with experimental apparatus.

The author would like to thank his colleagues Mr. Bill Pugh, Mr. Kevin Dahil and Mr. Bashir Sayar for help with the experimental investigation and for discussions of the problem.

This work is dedicated to the author's parents and elder brothers for their concern, personal sacrifice, and wise counseling which provided both the opportunity and climate for this educational experience.

TABLE OF CONTENTS

LIST OF TABLES

LIST OF ILLUSTRATIONS

NOMENCLATURE

		Units
A_o	Area of an orifice	$in.^2$
A_p	Area of a piston	$in.^2$
d_o	An orifice diameter	in.
D	d/dt	
F	Force	lbf.
F_f	Coulomb friction force	lbf.
g_o	Conversion factor, (385.9)	$lbm\text{-}in./lbf\text{-}sec.^2$
I	Inertia of rotating parts which move rigidly with the Pawl	$lbm\text{-}in.^2$
K	Spring stiffness	lbf/in.
M	Total mass of the system	lbm.
M_{eq}	Equivalent mass of rotating parts which move rigidly with the pawl	lbm.
M_p	Mass of the piston	lbm.
N	Normal force acting between the piston and the cylinder surface	lbf.
P	Pressure	$lbf/in.^2$
r_p	Radius of the piston	in.
r	Radius of the ratchet	in.
V	Velocity	in/sec.
Z	Damping factor for an orifice	$lbf\text{-}sec^2/in.^2$
ρ	Mass density of air	$lbm/in.^3$
μ	Coefficient of friction	
ν	Dynamic viscosity	$lbf\text{-}sec/in.^2$

ℓ	Length of the piston	in.
a	Distance, as defined in Figure 4	in.
b	Distance, as defined in Figure 4	in.
c	Clearance between the piston and the cylinder	in.
b_o	Distance between mid-point of the piston and point A, see Figure 4, when the spring is in free position	in.

SUMMARY

The objective of this study is to analyze a damped escapement mechanism in which fluid damping with air as the damping medium is provided by an orifice, annular clearance between the piston and the cylinder, and dry friction between the piston and the cylinder surface.

The response curves of the system are obtained theoretically and experimentally as a function of design parameters. Experimental and theoretical curves may be seen to give fair agreement. While the mathematical model encompasses simplifying assumptions, its simplicity recommends it for design purposes.

CHAPTER I

INTRODUCTION

It is frequently necessary for machine parts to operate intermittently instead of continuously, and there are various forms of mechanisms for obtaining these intermittent motions. One of the simplest and most common methods of obtaining intermittent motions is by means of escapement. The escapement mechanism, for example, is used for operating a paper feed-roll used in connection with a printing unit of a machine or is incorporated in a wire weaving machine to advance strands of wire a required distance at regulated time intervals. An escapement may be considered as a form of ratchet mechanism having an oscillating pawl for controlling the motion of the ratchet wheel by engaging successive teeth. Since pawl and wheel are not connected positively, the pawl hits the teeth of the wheel abruptly. The aim of this investigation is to analyze a system which would absorb the abrupt force.

Statement of the Problem

The objective of the study is to analyze a damped escapement mechanism, shown in Figure 1, which employs an orifice as a damping device and air as the damping medium. A response of the system as a function of design parameters is investigated.

Method of Analysis

The procedure followed in this study is one of theoretical analysis

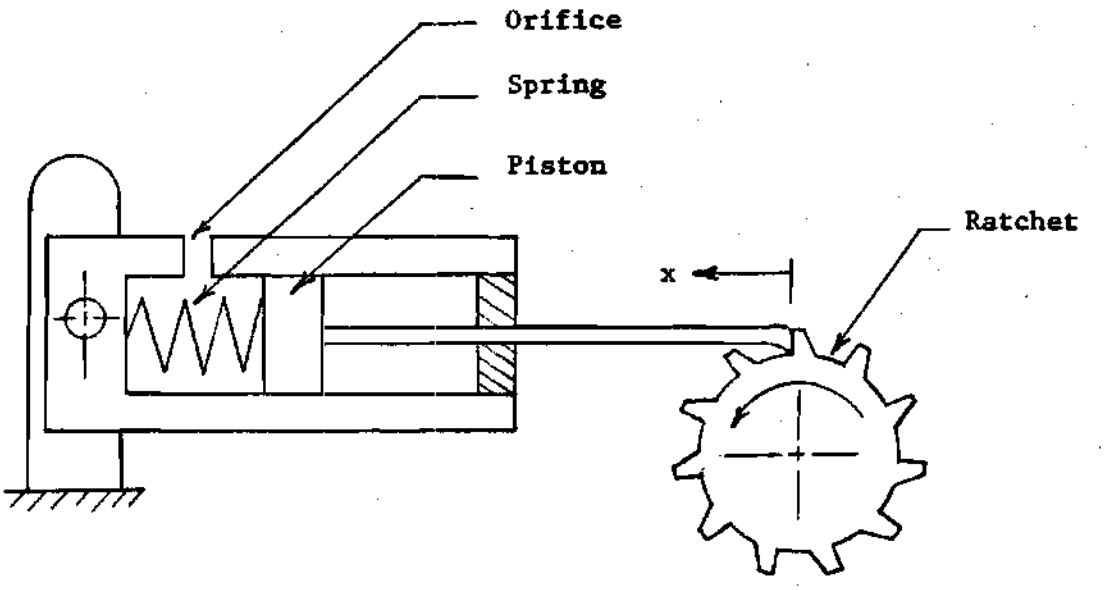

Figure 1. Schematic Diagram of a Damped Escapement Mechanism

and experimental verification. First the problem is treated analytically on the analog computer and then the results are verified by experimental techniques. The response curves as a function of design parameters are obtained.

Although the orifice-type damper is one of the most widely used methods of dissipating kinetic energy or limiting velocity in a mechanical system, a search of existing literature revealed that little has been done in the area of correlating experimental data and developing design procedures from it.

Buzzard (1)* has done work on an orifice type damper having harmonic excitation and has investigated frequency response. Silveira et al. (2) have done an experimental investigation for a number of different designs of small fluid displacement or viscous shear dampers suitable for dynamic model application. The damping characteristics of the dampers tested, of different design geometries, exhibited three general trends: a) the damping force increased approximately linearly as the maximum piston velocity increased, b) the damping force varied approximately as the square of the maximum piston velocity, and c) the damping force varied approximately as the square root of the maximum piston velocity. Jacobsen (3) has derived a general method of obtaining approximate solutions of the steady forced vibrations of a damped system of one degree of freedom with various types of damping for the case of sinusoidally varying disturbing forces. The approximation consists in expressing all

---

* Numbers in parentheses refer to the Literature cited at the end.

the dampening terms of the original differential equation by a single equivalent damping term, proportional to the first power of the velocity of system.

CHAPTER II

THEORETICAL INVESTIGATION

A schematic diagram of a damped escapement mechanism is shown in Figure 1 and a mathematical model is shown in Figure 2. Damping in the system is provided by an orifice, annular clearance between the piston and the cylinder, and dry friction between the piston and the cylinder surface.

During this work, it has been found that for the model constructed, shown in Appendix-I, the damping due to clearance is negligible. Thus it is necessary to take account of only orifice damping and coulomb damping which is due to dry friction. An extensive argument of this point is given in Appendix-II.

Fluid Mechanics of an Orifice Type Damper

A simple model of the damping device is shown in Figure 3. The following stipulations about the damper are made:

1. The damping medium is an ideal, frictionless fluid.

2. The orifice diameter is sufficiently smaller than the piston diameter so as to make the velocity through the orifice much greater than the piston velocity.

3. The integrated form of the Bernoulli equation is applicable.

On the basis of the third assumption, the following relation holds true:

$$(P_1 - P_2) = (V_2^2 - V_1^2) \frac{\rho}{2g_o} \qquad (1a)$$

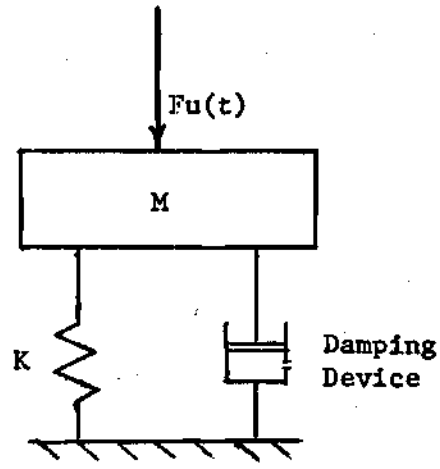

Figure 2. Mathematical Model of the Damped Escapement Mechanism

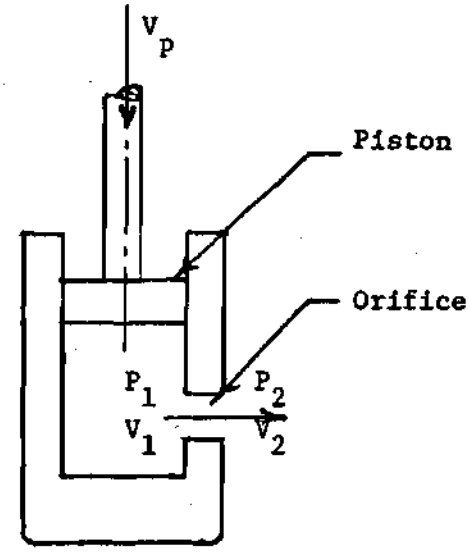

Figure 3. Orifice Type Damper

The damping force will then be

$$F = (P_1 - P_2)A_p = (V_2^2 - V_1^2)\frac{\rho A_p}{2g_o}$$

As a result of assumption two, V_2^2 is much greater than V_1^2 and therefore

$$F = V_2^2 \rho A_p / 2g_o$$

From the consideration of continuity, assuming incompressibility,

$$A_p V_p = A_o V_2 \qquad \text{or} \qquad V_2 = (A_p/A_o)V_p$$

therefore

$$F = V_p^2 \rho A_p^3 / 2g_o A_o^2 \qquad (1)$$

or, Damping Factor

$$Z = F/(Dx)^2 = F/V_p^2 = \rho A_p^3 / 2g_o A_o^2$$

In the preceding two equations it should be noted that V_2 and A_2 have been replaced by V_o and A_o since it is customary to locate point 2 just beyond the orifice, and by so doing, it represents a point where the pressure is that of the atmosphere but where the air jet has the velocity and area found at the throat of the orifice.

It should be noted that the damping force as defined by Equation (1) is proportional to the square of the piston velocity and 180 degrees out of phase with it.

Equation of Motion

The differential equation of motion for the system shown in Figure 2

can be written as follows:

$$MD^2x = Fu(t) - Kx \pm Z(Dx)^2 \pm F_f \tag{2a}$$

Rearranging Equation (2a) gives

$$MD^2x \pm Z(Dx)^2 \pm F_f + Kx = Fu(t) \tag{2}$$

The input force on the system is assumed to be a step force; this assumption is verified experimentally.

Assuming a rigid contact between the piston rod and the ratchet, a value of mass M in Equation (2) is

$$M = M_p + M_{eq}$$

where M_{eq} is the equivalent mass of rotating parts which move rigidly with the piston rod.

The value of M_{eq} is found from kinetic energy considerations as follows:

$$\tfrac{1}{2} I (D\theta)^2 = \tfrac{1}{2} M_{eq} (Dx)^2$$

Using the relation

$$Dx = rD\theta$$

one obtains

$$M_{eq} = I (1/r)^2 \tag{3}$$

An estimation of the value of F_f was done as follows: There is a tendency for the piston rod to cock in its guide due to eccenticity of the

load. If point A, see Figure 4, is the pivot point assumed, then the distance between the pivot and mid-point of the piston can be expressed as $(b_o + x)$. The normal force N could be found from

$$N = \left(\frac{a}{b_o + x}\right)F$$

and hence,

$$F_f = \mu N = \left(\frac{\mu a}{b_o + x}\right)F \qquad (4)$$

Theoretical Solution

The $(Dx)^2$ term in the equation of motion causes the equation to be nonlinear. The method of equivalent viscous damping is one of the methods to obtain an approximate solution. In attempting to solve an equation involving a nonlinear damping device by the method of equivalent viscous damping, the procedure is to replace the nonlinear device with an equivalent linear device. The equivalence of the linear devices is judged on the amount of energy absorbed per cycle under harmonic excitation (4). Since the method of equivalent viscous damping is limited for harmonic excitation, it was desirable to seek other means of solution. Since the electronic analog computer lends itself to the rapid solution of differential equations, it was selected for the work. The analog computer circuit shown in Figure 5 is the one which was used. The results obtained are shown in Chapter IV.

Appendix-III gives the details of the analog program.

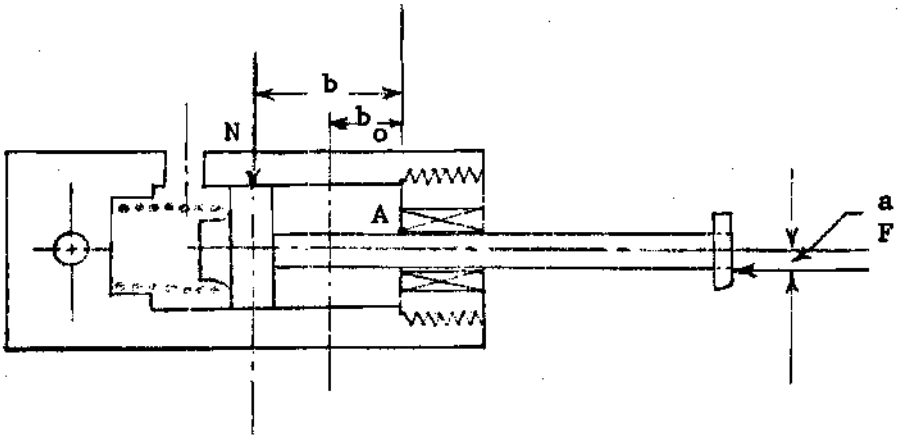

Figure 4. Details for Estimating Coulomb Friction Force

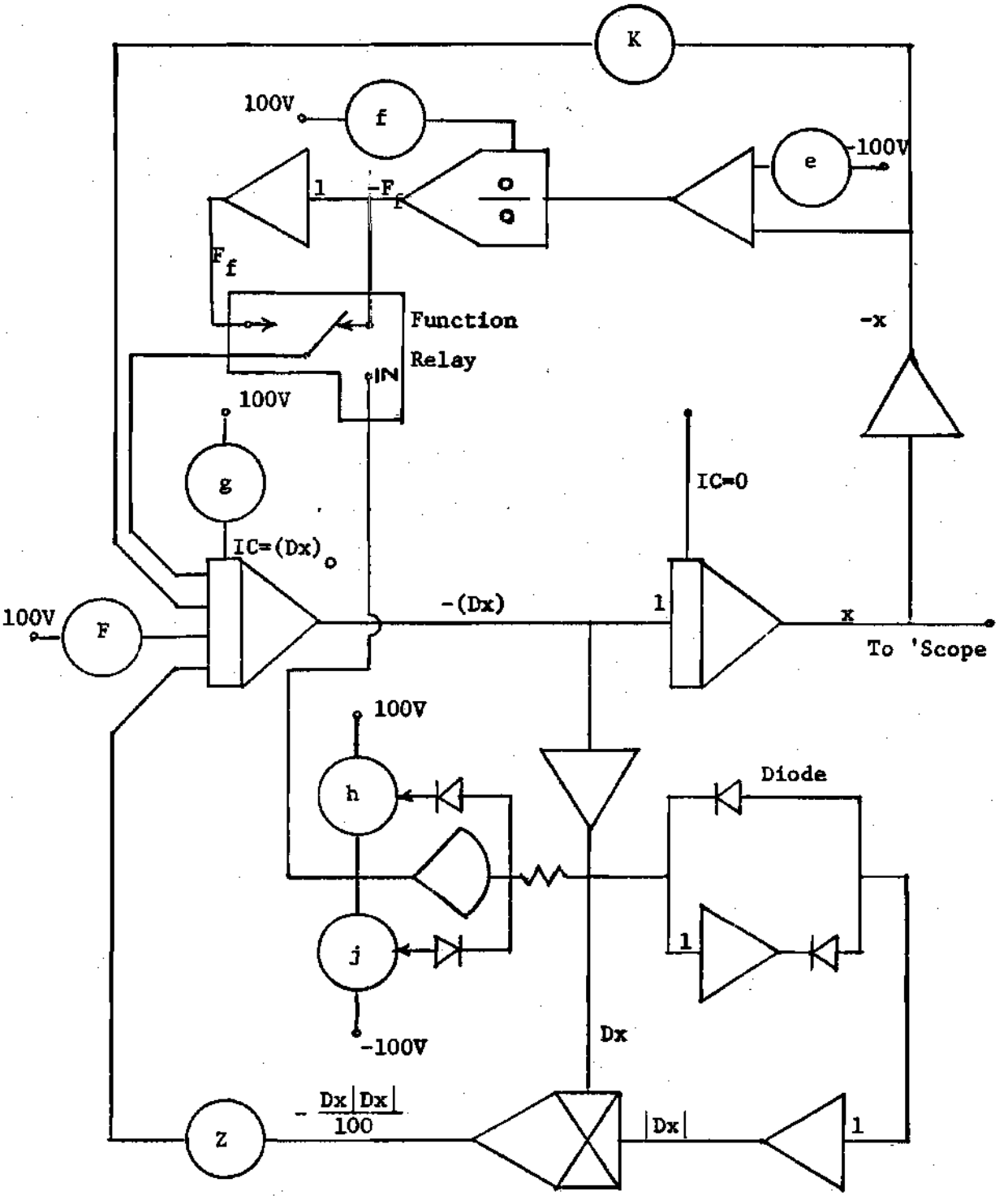

Figure 5. Analog Computer Circuit for the Damped Escapement Mechanism

CHAPTER III

EXPERIMENTAL INVESTIGATION

To quantitatively establish the correspondence between the mathematical model and a real escapement system, an experimental set-up was designed and instrumented to record correlative data. A schematic diagram of the model set-up is shown in Figure 6 and details of the pawl-damper are given in Appendix-I. When the pawl-damper is dropped onto the ratchet, all units on the output side of the slip clutch, including the piston and the ratchet, are assumed to move as a rigid body. For better understanding of the following discussion, the reader is advised to study Figure 6 carefully. The damped escapement model was designed so that the orifice sizes and the springs could be easily changed.

Instrumentation and Equipment

The instrumentation consists of transducers that are attached to the experimental model and of readout equipment. The angular vibrations of the ratchet are measured by a light and photocell unit. The force acting on the piston rod is evaluated from strain gage output. The data obtained from the experimental model are in the form of oscillographs.

The various equipment used for the experiments are listed below in Table 1.

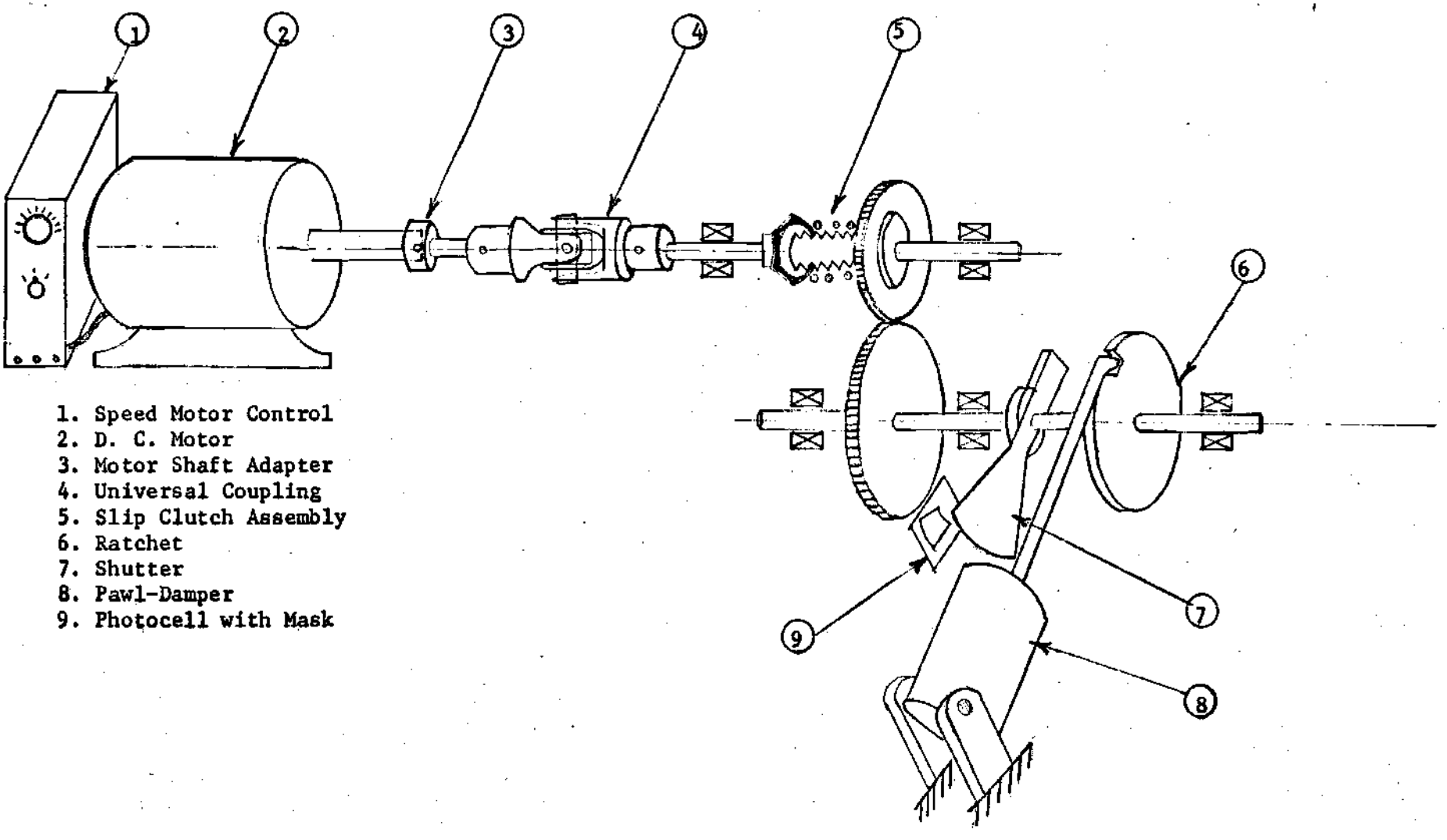

1. Speed Motor Control
2. D. C. Motor
3. Motor Shaft Adapter
4. Universal Coupling
5. Slip Clutch Assembly
6. Ratchet
7. Shutter
8. Pawl-Damper
9. Photocell with Mask

Figure 6. Experimental Set-up

Table 1. Experimental Equipment

Item	Manufacturer	Specifications
Battery Eliminator	Heathkit	IP-12
Bridge Amplifier	Ellis Associates	BAM-1
Filter	- - -	FV-1
D. C. Motor	Bodine	NSH-54
Motor Speed Control	Minarik	SH-53
Oscilloscope	Tektronix	Dual Beam type 502A
Oscilloscope Camera	Tektronix	Polaroid type C-27

Angular Displacement Transducer

A light sensitive transducer was used to obtain the response curves for the dynamic system. A selenium photovoltaic cell was attached to a stationary support and illuminated by a constant intensity light source. The rotating shutter was located between the light and the photocell and thereby cast a shadow on the cell. As the system and its shadow were displaced, the illuminated area of the photocell changed and the resulting voltage change was related to the displacement of the system.

The photocell that was used was essentially a P-N type transistor which produces an electrical voltage when illuminated. For a stronger light intensity or a larger illuminated area, the voltage output of the

cell was higher. Figure 7 shows the circuit which was employed with the photocell.

The battery provided a reversed bias across the photocell which improved both its linearity and the magnitude of its output. A shutter of wedge shape with aperture, as shown in Figure 9, with its center at the center of the shaft was used to get linear calibration. The output of this transducer circuit was displayed on an oscilloscope.

The light source consisted of a single bulb powered by a d.c. voltage source; all the tests were conducted in a darkened room to insure a constant illumination. A frosted lens was used to smooth out the light's intensity and thereby eliminate the bright spot.

To take advantage of the linearity of the photocell's voltage output, the following procedure was followed before the cell was calibrated:

1. The entire area of the photocell was illuminated with the desired light intensity.

2. The gain potentiometer, Figure 7, was adjusted until the output voltage was zero.

3. The gain potentiometer resistance was lowered slightly further to move away from the point of zero output voltage..

4. Care was taken not to overdo this last step as it tended to reduce the photocell's output voltage.

A worm and worm wheel arrangment with a disc dial was used to measure angular displacement of the ratchet shaft and thus for calibration of the photocell. A calibration curve was obtained by plotting this angular displacement versus the corresponding voltage from the photocell. As can be seen in Figure 8, this voltage angular displacement relationship

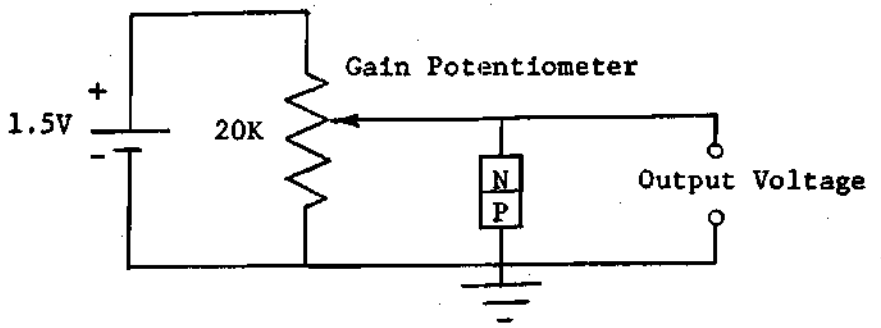

Figure 7. Photocell Angular Displacement Transducer Circuit

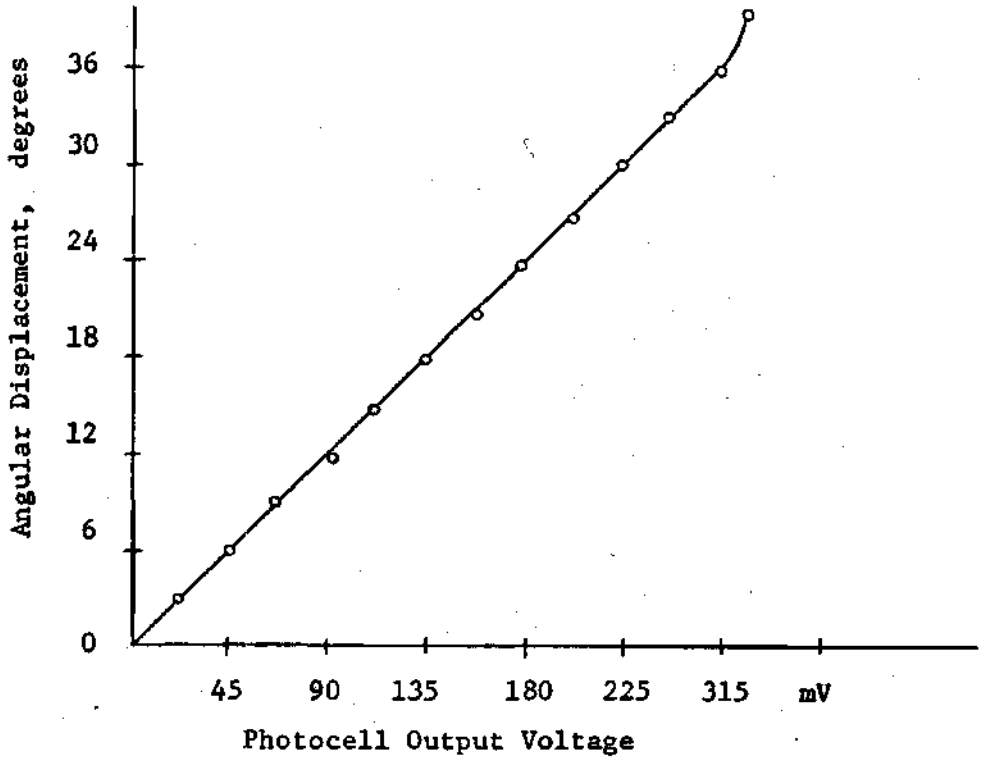

Figure 8. Typical Photocell Calibration Curve

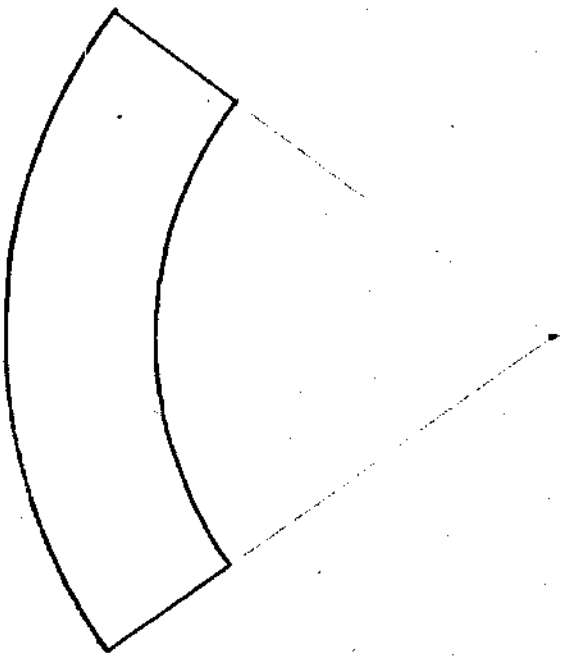

Figure 9. The Shape of the Aperture used to Mask the Photocell

is linear. A linear displacement of the piston rod can be obtained from this, since it is assumed that the ratchet and the piston rod move rigidly.

Force Transducer

A strain gage was mounted on the piston rod by wrapping around on the surface and a change in resistance of the gage on application of force was obtained as a signal proportional to the force. The gage used was constructed with a foil grid mounted on a very thin epoxy plastic film and was mounted with an epoxy cement of the thermosetting type. The procedure used was as follows:

1. The piston rod and the gage surface were cleaned with trichloroethylene. The gage was handled with tweezers at this point to prevent contamination.

2. An epoxy cement was employed, which was prepared from resin and hardener at the time of use. A generous coating of the cement was applied to the piston rod surface, using care to eliminate any air bubbles. The gage was positioned with grid facing upward and air bubbles as well as excess cement were removed from under the gage. A piece of teflon paper was placed over the gage and pressure of 5 to 10 psi. was applied while the cement was curing. Teflon paper was used because the cement does not adhere to it. A 24 hour curing time was required.

A schematic diagram of the force measuring circuit is shown in Figure 10, which basically employs one active arm of a wheatstone bridge circuit. The band pass filter was used to get rid of random high frequency noise.

The strain gage was calibrated by applying static torque on the

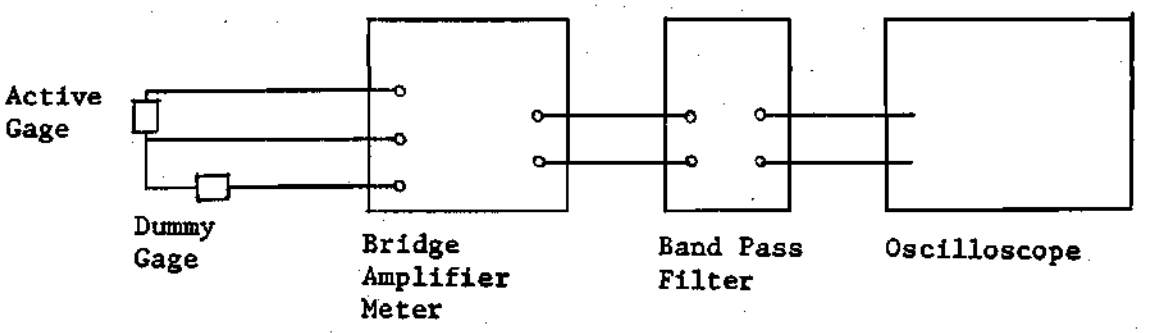

Figure 10. Strain Gage Force Transducer Circuit

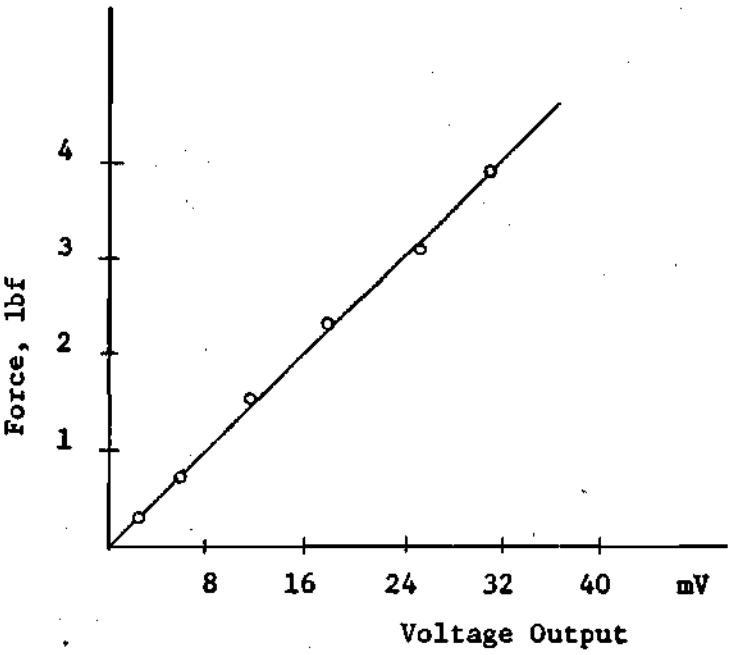

Figure 11. Typical Strain Gage Calibration

ratchet shaft by means of a dead weight hanging over one end of a pulley mounted on the shaft. A force acting on the piston rod was calculated from the dead weight and was plotted against voltage output from the strain gage circuit. The calibration curve as shown in Figure 11 is linear.

The force acting on the system is assumed to be a step input force and the assumption was experimentally verified to be valid. The step force, converted in terms of torque on a clutch, is equal to the slip torque of the clutch. Since the slip torque of the clutch can easily be found by gradually applying static torque on the ratchet shaft, this torque measurement was used as a check against the value obtained from the strain gage output.

Because of the small strain in the piston rod, voltage output from the strain gage circuit was quite small and hence electrical noise was quite predominant. Methods for eliminating electrical noise are enumerated below:

1. Use shielded cables.

2. The transducer leads must be independent of the shield.

3. The shields on the cables as well as the part under test should all be grounded at the oscilloscope.

4. Try to keep the transducer leads and equipment out of strong electromagnetic fields.

5. Twisting all leads together often reduces electromagnetic pick-up.

6. Extra shielding of aluminum foil placed over leads and transducer does help.

7. Noisy 'scope signal may be due to poor contact in jacks.

CHAPTER IV

RESULTS AND DISCUSSION

The numerical results of the theoretical analysis of Chapter II and the experimental results of Chapter III are now evaluated and compared.

Comparison of the Theoretical and Experimental Response Curves

The main objective of the investigation is to relate response to the design parameters of the system, mainly to orifice diameter. Comparison of experimental and and theoretical response curves is presented in Figures 12 to 15. Experimental and theoretical curves may be seen to give fair agreement. While the mathematical model encompasses simplifying assumptions, its simplicity recommends it for design purposes.

A few comments on the response curves in Figures 12 to 15 are enumerated below:

1. The theoretical and experimental locations of first peak agrees well for each orifice.

2. The observed and predicted initial slopes are in fairly good agreement.

3. The experimental results show no oscillations. It should be noted that the physical system is modeled as a single degree of freedom system for the sake of simplicity. It is suggested that shaft flexure at the ratchet introduces additional friction caused by bearing misalignment. This could be more adequately described in a two degree of freedom model.

4. A response curve with maximum spring stiffness should have the

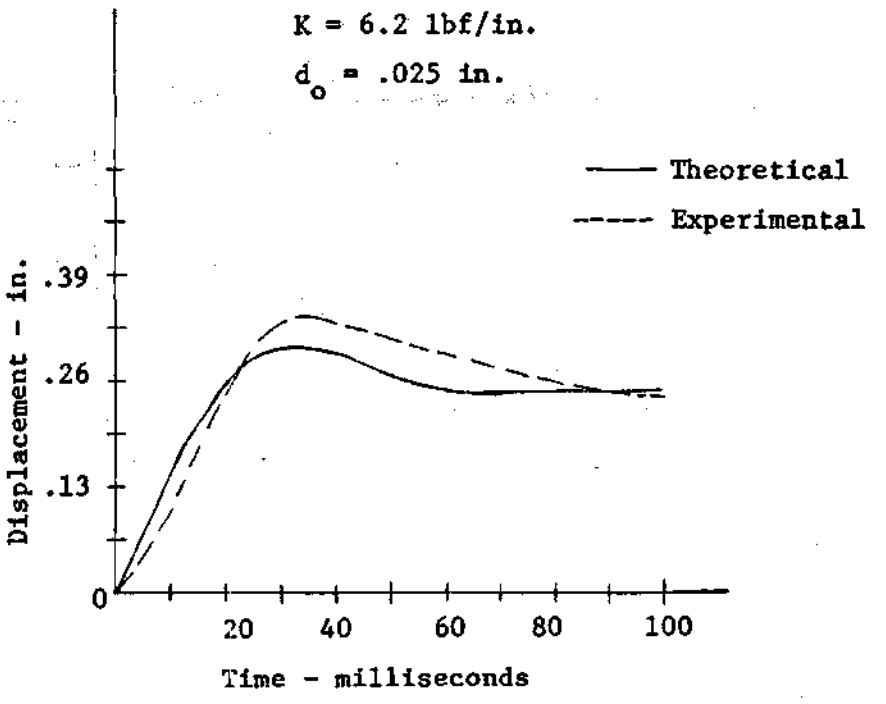

Figure 12. Comparison of Theoretical and Experimental Response Curves

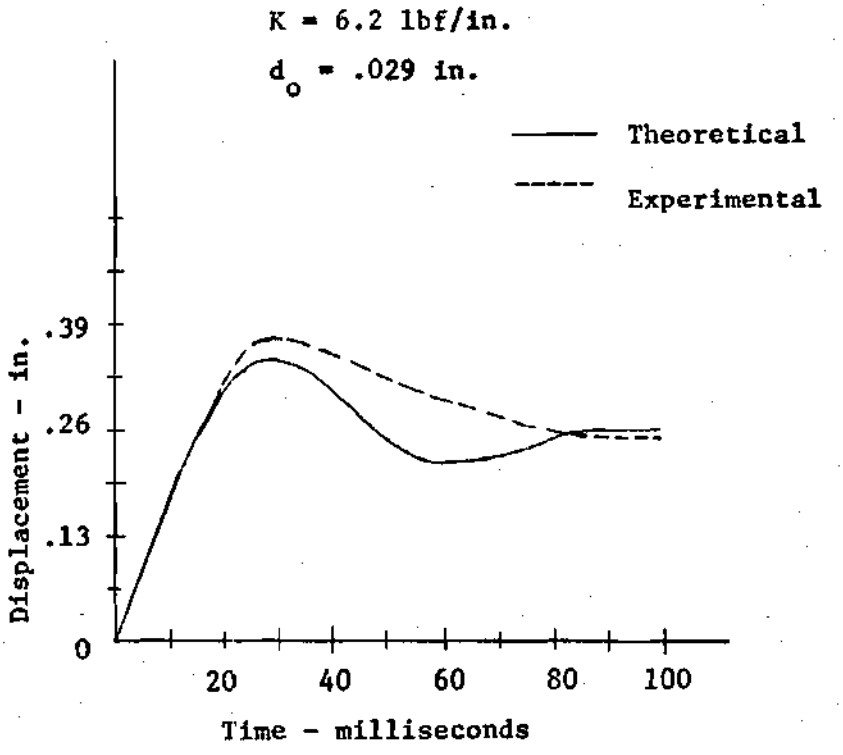

Figure 13. Comparison of Theoretical and Experiment Response Curves

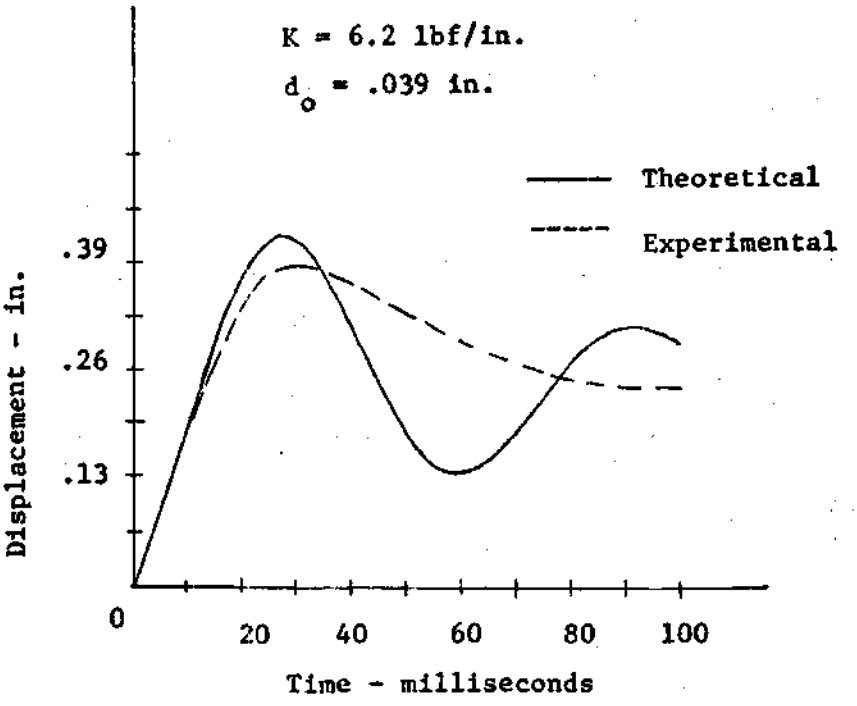

Figure 14. Comparison of Theoretical and Experimental Response Curves

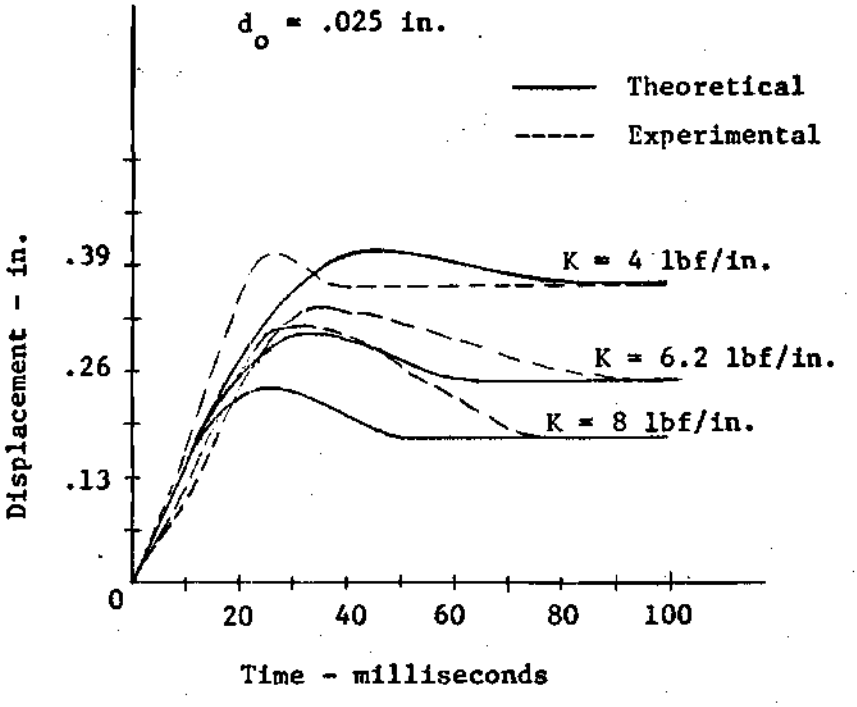

Figure 15. Comparison of Theoretical and Experimental Response Curves for Different Spring Stiffnesses

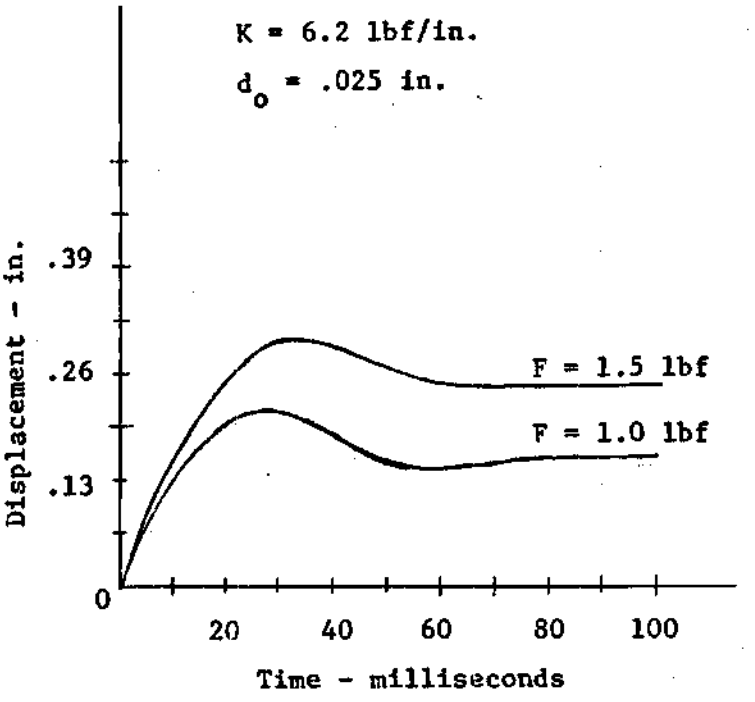

Figure 16. Theoretical Response Curves for Different Forcing Functions

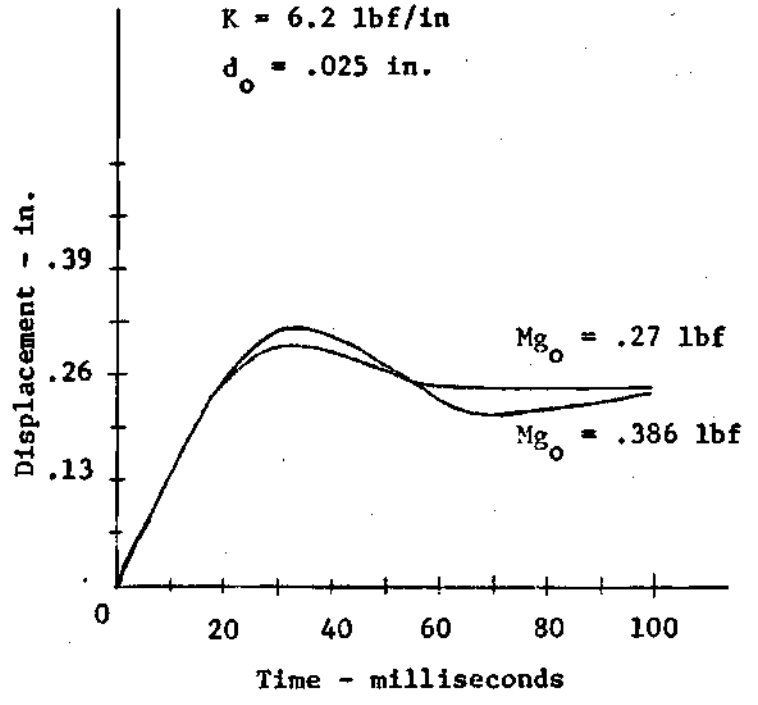

Figure 17. Theoretical Response Curves for Different Masses

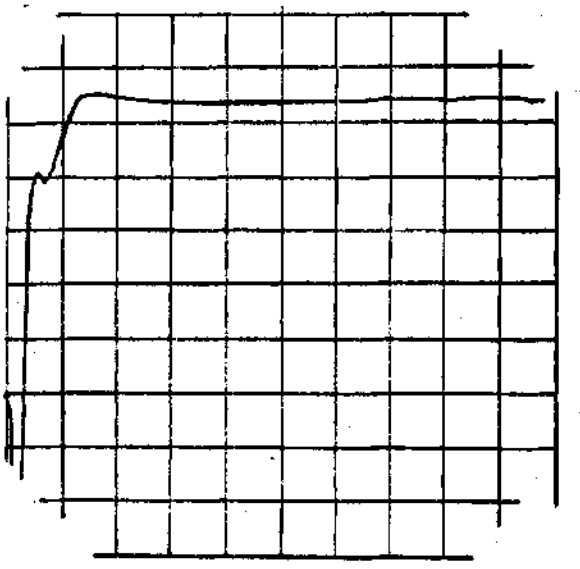

Figure 18. Typical Oscilloscope Record of the Strain Gage Output

shortest time to peak displacement. The predicted response has the proper trend. This is not the case with the observed response.

The theoretically predicted curves for different values of force and mass acting on the system are shown in Figures 16 and 17. An increase of the force increases the steady state height, as expected. An increase of mass results in the longer time to first peak displacement, as expected.

Figure 18 shows a typical strain gage output showing verification of the assumption that the forcing function on the system is a step input force.

CHAPTER V

RECOMMENDATIONS

The following recommendations are made concerning possible areas of future investigation:

1. The possibility of uncovering, in the case of a nonlinear device, a concept similar in nature to damping ratio for a linear device. At the moment, the possibility seems quite remote, but in as much as the solution for a system must be carried out on a computer, it would seem highly desirable to find some way of relating the response of such a system to its physical parameters such that it would be unnecessary to perform the complete solution for each problem encountered.

2. The possibility of getting response curves as a function of nondimensional ratios.

3. To study response curves with orifice(s) in the piston itself.

4. The possibility of extending the work to include noncircular orifices.

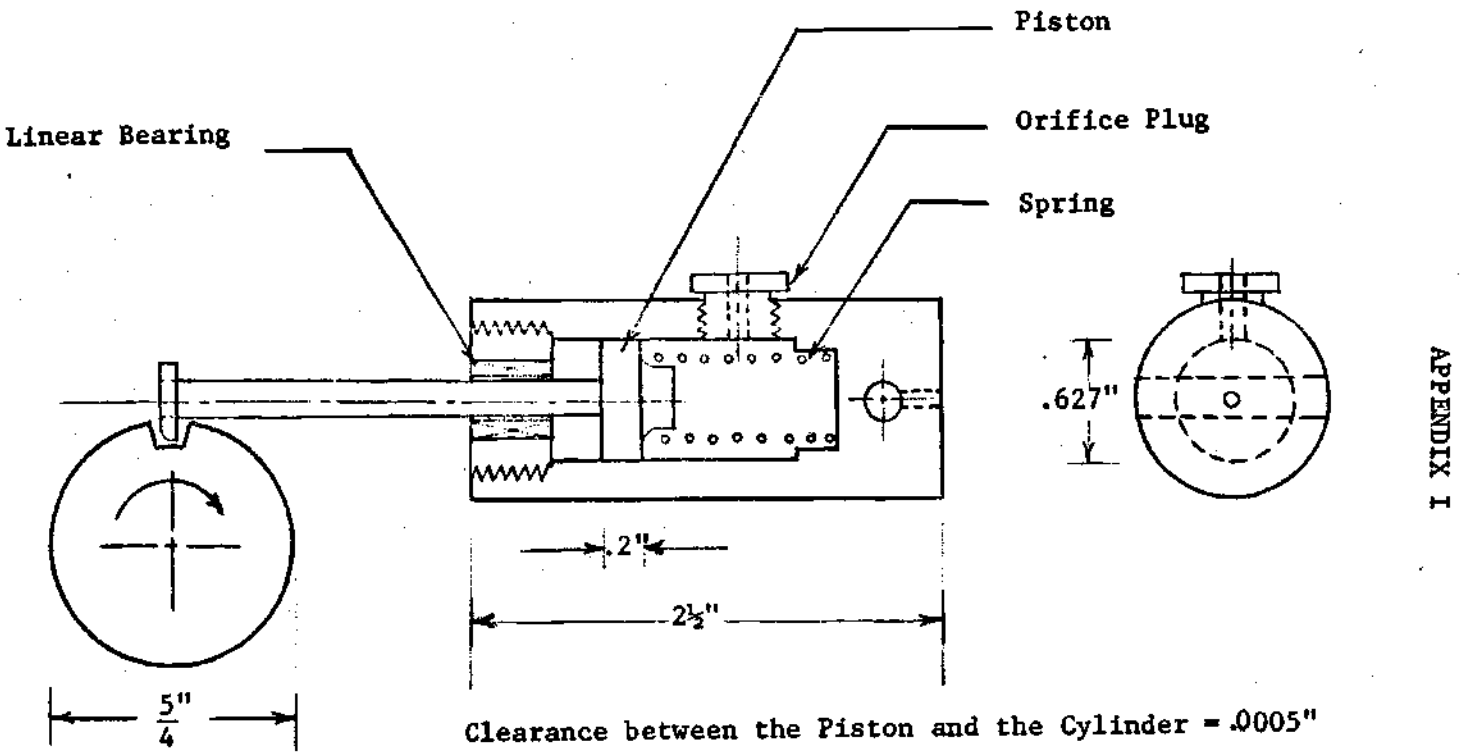

Figure 19. A Detailed Sketch of the Pawl-Damper

APPENDIX II

DAMPING EFFECT DUE TO CLEARANCE

It is intended to show here that the damping effect due to clearance for the pawl-damper model constructed is negligible.

Consider a damping due to clearance between the piston and cylinder.

Assuming laminar flow, the velocity gradient between the piston and the cylinder shown in Figure 20 can be written as

$$\frac{dv}{dy} = \frac{\Delta P}{\nu \ell} (h - y)$$

Integrating,

$$v = \frac{\Delta P}{\nu \ell} (h - y^2/2)$$

The toal volume of flow is

$$V = 2\pi r \int_{-h}^{+h} v dy$$

Integrating and writing in terms of the clearance gives

$$V = \frac{\Delta P}{\nu \ell} \, \epsilon^3 r \qquad (A.1)$$

From equation (1) of Chapter II, with orifice as the damping device,

$$F = \Delta P A_p = V_2^2 \, \rho \, A_p / 2 g_o \qquad (A.2)$$

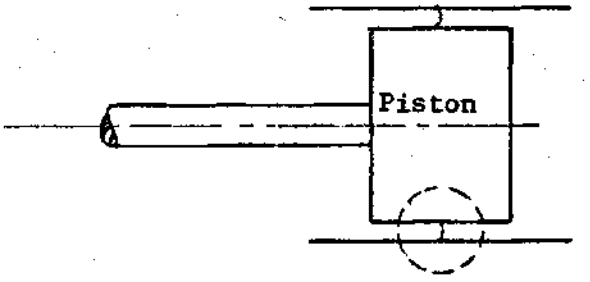

(a)

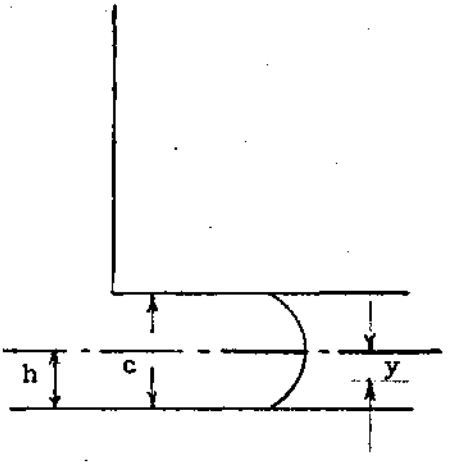

(b)

Enlarged view of dotted area in (a)

Figure 20. Damping Due to Clearance

From the consideration of continuity, assuming incompressibility, one can write

$$A_p V_p = A_o V_2 + A_{clearance} \; V_{clearance} \tag{A.3}$$

The second term on the right hand side of equation (A.3) is nothing but the expression (A.1). From equation (A.2),

$$V_2 = \left(\frac{2g}{\rho} \Delta P\right)^{\frac{1}{2}} \tag{A.4}$$

Substituting (A.1) and (A.4) in expression (A.3)

$$A_p V_p = \sqrt{\Delta P} \; \left(A_o^2 \; \frac{2g_o}{\rho}\right)^{\frac{1}{2}} + \Delta P \; \left(\frac{\pi c^3 r}{\nu \ell}\right) \tag{A.5}$$

Using d = .029 inch, c = .0005 inch and other numerical values for the model, the equation (A.5) becomes

$$A_p V_p = \sqrt{\Delta P} \;\; 3.09 + \Delta P \;\; .001645 \tag{A.6}$$

It should be noted that the equation (A.6) is valid for the choice of parameters for the model constructed. The values of ΔP existing in the model are such that the last term in the equation (A.6) can be neglected. Thus, one can conclude that most of the air passes through the orifice and negligible amount through the clearance, which means that the damping effect due to clearance is negligible.

APPENDIX III

ANALOG PROGRAM

The equation of motion for the damped escapement mechanism is

$$MD^2x \pm Z\,(Dx)^2 \pm F_f + Kx = Fu(t) \qquad (A.7)$$

The numerical data for the system are:

Mg_o = .27 lbf.

r_p = .627 in.

ρ/g_o = .00192 lbf-sec^2/ft^4 at room temperature

a = .0937 in.

b = .41 in.

μ = .42

F = $1.5\varepsilon_3$ lbf. $\qquad 0 \leq \varepsilon_3 \leq 1$

K = $10\varepsilon_2$ lbf/in. $\qquad 0 < \varepsilon_1 \leq 1$

d = $.029\varepsilon_o$ in. $\qquad 0 < \varepsilon_o \leq 1.5$

The numerical values give:

$$Z = .0312/\varepsilon_o^4 = .00312\varepsilon_1 \text{ lbf-sec/in.}$$

(Letting $\varepsilon_1^4 = 1/\varepsilon_o^4$)

$$F_f = .059/(.41 + x) \text{ lbf.}$$

Substituting these numerical values in the equation (A.7), one obtains

$$.0007D^2x \pm .00312\varepsilon_1(Dx)^2 \pm .059/(.41+x) + 10\varepsilon_2 x = 1.5\varepsilon_3 \qquad (A.8)$$

Since the orifice damping force always opposes the piston motion, the $(Dx)^2$ term which appears must really be formed as the product of Dx and the magnitude of Dx, i.e. $|Dx|Dx$. The Coulomb friction force also always opposes the piston motion.

Using time scale factor, n = 100 and magnitude scale factors,

$$a_x = a_{Dx} = a_{D^2x} = 100$$

the equation (A.8) reduces to

$$(100D^2x) + .0446\varepsilon_1(100Dx|100Dx|) \pm 84.37/(41+100x) + 1.43\varepsilon_2(100x) = 21.42\varepsilon_3 \quad \text{(A.9)}$$

The reader is requested to refer to a suitable text (5) for details of method of arriving at equation (A.9).

The analog circuit for obtaining the solution to equation (A.9) is presented in Figure 21.

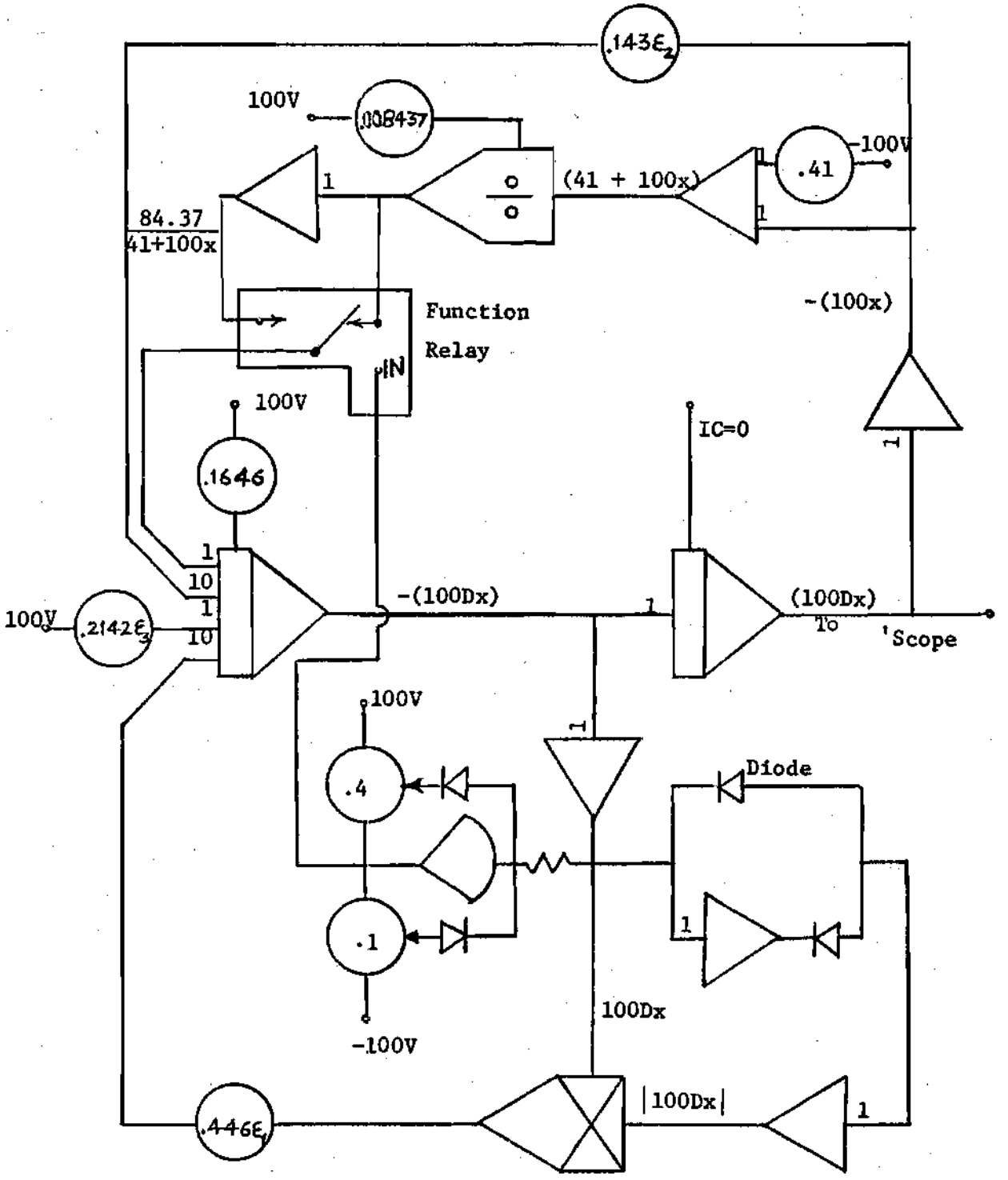

Figure 21. Analog Circuit for the Damped Escapement Mechanism

BIBLIOGRAPHY

Literature Cited

1. G. H. Buzzard, "The Dynamic Response of a Nonlinear Hydraulic Damping Device," ASME Publication 61-WA-205.

2. M. A. Sileira, D. J. Maglieri, and G. W. Brooks, "Results of an Experimental Investigation of Small Viscous Dampers," NACA TN 4257, June 1958.

3. L. S. Jacobsen, "Steady Forced Vibration as Influenced by Damping," APM-52-15 ASME Trans. pp. 169-180.

4. J. N. Macduff and J. R. Curreri, Vibration Control, McGraw-Hill, 1958.

5. G. R. Peterson, Basic Analog Computation, The MacMillan Company, 1967.

Other References

1. H. N. Norton, Handbook of Transducers for Electronic Measuring Systems, Prentice-Hall, Inc., 1969.

2. John Sasuga, Solar Cell and Photocell Handbook, International Rectifier Corporation.

3. T. G. Beckwith and N. L. Buck, Mechanical Measurements, Addison-Wesley Publishing Company, Inc., 1963.

4. "Calculating Damping Factors for Dashpot Dampers," Product Engineering, Vol. 27, April 1956, pp. 162-165.